Available on the CERN CDS information server **CMS PAS HIG-14-012**

CMS Physics Analysis Summary

Contact: cms-pag-conveners-higgs@cern.ch 2014/07/03

Constraints on Anomalous HWW Interactions using Higgs boson decays to W+W- in the fully leptonic final state

The CMS Collaboration

Abstract

Studies on anomalous Higgs boson interactions with pairs of W gauge bosons, as well as its spin parity are presented. The analysis is performed in the Higgs boson decay channel to W^+W^- with two charged leptons, one electron and one muon, and two neutrinos in the final state. The analysis is based on data recorded with the CMS detector in pp collisions at a center of mass energy of 8 TeV at the LHC. The tensor structure of interactions under the spin-0 hypothesis is examined and alternative spin-parity hypotheses are studied to cover the spin-1 and spin-2 models. The hypothesis of the standard model Higgs boson for quantum numbers and couplings is consistent with the data and the results are expressed as exclusion bounds of several spin-parity hypotheses and anomalous coupling parameters.

1 Introduction

The ATLAS and CMS experiments at the Large Hadron Collider (LHC) reported the discovery of a new boson [1–3] with a mass of approximately 125 GeV using data from proton-proton collisions at a center of mass energy of 7 and 8TeV in 2012. So far, the observation is compatible with a Standard Model (SM) Higgs boson at that mass. The spin-parity of the boson has been studied since and the observation is so far consistent with the pure scalar hypothesis when compared to several other spin-parity hypotheses [4–6].

In particular, CMS performed a final measurement of the Higgs boson decaying to a W-boson pair [5] using the full dataset recorded during the Run-I of the LHC at $\sqrt{s}$ =7 and 8 TeV. An excess corresponding to a significance of 4.3 standard deviations was reported in this channel for $m_{\mathrm{H}} = 125.6$ GeV, reference mass that will be used in this note from now on. A first study of the spin-parity was performed within this measurement. The $J^P = 0^+$ hypothesis was favoured against a narrow resonance with $J^P = 2^+$ or 0^- decaying to a W-boson pair.

However, detailed measurements of the properties of the new boson still need to be performed in order to determine if it is indeed a SM particle. To precisely measure its quantum numbers, mass, and couplings to SM fields is of high interest at the LHC experiments. Phenomenological studies have been presented in Refs. [7–13]. This note reports the study of the spin parity and tensor structure of the Higgs boson following the strategy proposed in [11, 13]. The work presented in [5] is extended by increasing the number of scenarios studied. In [5], the alternative scenarios of $J^P = 2^+$ and 0^- where studied, here nine additional J = 2 and three J = 1 exotic scenarios are explored. In addition to testing pure J^P states against the SM Higgs boson hypothesis, a fit for a continuous parameter f_{a3}^{WW} (as well as f_{a2}^{WW} and $f_{\Lambda 1}^{WW}$, defined in Eq.4), related to anomalous couplings of the Higgs boson, is performed for the first time in this channel, following what was done in [6] for $\mathrm{H} \to ZZ$.

The analysis aims to perform, in the context of $\mathrm{H} \to \mathrm{W}^+\mathrm{W}^-$ decays, and together with $\mathrm{H} \to ZZ$ [14], the experimental determination of all helicity amplitudes involving a Higgs boson decaying to two gauge bosons and extract all the possible information on spin-parity and HVV (V=Z,W) couplings from the Run-1 data at 7 and 8 TeV.

The analysis strategy is based on the final state of $\mathrm{H} \to \mathrm{W}^+\mathrm{W}^-$ decays in which both W bosons decay leptonically, resulting in a signature with two isolated, oppositely charged, high p_{T} leptons (electrons or muons) and large missing transverse energy, $E_{\mathrm{T}}^{\mathrm{miss}}$, due to the presence of undetected neutrinos. In this channel, observables such as the opening angle between the two reconstructed leptons in the transverse plane, the dilepton invariant mass, and the transverse mass, have been shown to be optimal to discriminate between the SM Higgs boson hypothesis and other exotic resonances with different spin or parity [5].

The analysis inherits largely from the Run-I $\mathrm{H} \to \mathrm{W}^+\mathrm{W}^-$ paper [5] and has many common features with the $\mathrm{H} \to ZZ$ analysis [14] developed in parallel. The results obtained for $\mathrm{H} \to \mathrm{W}^+\mathrm{W}^-$ and $\mathrm{H} \to ZZ$ will be combined to extract the final information regarding spin parity and anomalous couplings of the Higgs boson using Run-1 data. The analysis presented here uses 19.4 ± 0.8 fb^{-1} of proton-proton collision data recorded by the CMS experiment at the LHC at $\sqrt{s} = 8$ TeV.

2 Tensor Structure and Spin Parity

The spin-0 J^P models 0^+, 0_h^+, and 0^- correspond to the terms with a_1, a_2, and a_3, respectively, appearing in the decay amplitude for a spin-0 boson defined as

$$A(H \to WW) = v^{-1} \left(\left[a_1 - e^{i\varphi_{\Lambda 1}} \frac{q_1^2 + q_2^2}{(\Lambda_1)^2} \right] m_W^2 \epsilon_1^* \epsilon_2^* + a_2 f_{\mu\nu}^{*(1)} f^{*(2),\mu\nu} + a_3 f_{\mu\nu}^{*(1)} \tilde{f}^{*(2),\mu\nu} \right) , \quad (1)$$

where $f^{(i),\mu\nu} = \epsilon_i^\mu q_i^\nu - \epsilon_i^\nu q_i^\mu$ is the field strength tensor of a gauge boson (W in decay or gluon in production in this analysis) with momentum q_i and polarization vector ϵ_i; $\tilde{f}_{\mu\nu}^{(i)}$ is the conjugate field strength tensor. Here, the amplitude coupling notation proposed in [11] is followed. Parity-conserving interaction of a pseudo-scalar corresponds to a_3, of a scalar to a_1, a_2, and Λ_1. The above sum retains only the leading terms in the q_i^2 expansion, which is therefore valid for small effective fractions of new contributions beyond the leading a_1 term. The SM Higgs coupling at tree level (to W^+W^-) is described by the a_1 term, while the a_2 term appears in the loop-induced processes, and as a small contribution due to radiative corrections in the W^+W^- couplings.

The couplings in Eq. (1) are generally complex form-factors which may depend on kinematic invariants, such as vector boson q^2. The lowest order in q^2 expansion, as shown in Eq. (1), is kept all couplings are assumed to be real in this analysis. Three fractions of the corresponding cross-sections (f_{a2}^{WW}, f_{a3}^{WW}, and $f_{\Lambda 1}^{WW}$) can describe the couplings, and three phases (ϕ_{a2}, ϕ_{a3}, and $\phi_{\Lambda 1}$) are assumed to be 0 or π, which are defined as follows

$$f_{a3}^{WW} = \frac{|a_3|^2 \sigma_3}{|a_1|^2 \sigma_1 + |a_2|^2 \sigma_2 + |a_3|^2 \sigma_3 + \sigma_4 / {\Lambda_1}^4} \; ; \; \phi_{a3} = \arg\left(\frac{a_3}{a_1}\right) \quad (2)$$

$$f_{a2}^{WW} = \frac{|a_2|^2 \sigma_2}{|a_1|^2 \sigma_1 + |a_2|^2 \sigma_2 + |a_3|^2 \sigma_3 + \sigma_4 / {\Lambda_1}^4} \; ; \; \phi_{a2} = \arg\left(\frac{a_2}{a_1}\right) \quad (3)$$

$$f_{\Lambda 1}^{WW} = \frac{\sigma_4 / {\Lambda_1}^4}{|a_1|^2 \sigma_1 + |a_2|^2 \sigma_2 + |a_3|^2 \sigma_3 + \sigma_4 / {\Lambda_1}^4} \; ; \; \phi_{\Lambda 1} \quad (4)$$

where σ_i is the effective cross-section of the process corresponding to $a_i = 1, a_{j\neq i} = 0$ (or $\Lambda_1 = 1$, $a_j = 0$). Given the measured value of f_x, it is possible to extract the coupling constants in any parameterization. For example, following Eq. (1) the couplings will be

$$\frac{|a_3|}{|a_1|} = \sqrt{\frac{f_{a3}^{WW}}{f_{a1}^{WW}}} \times \sqrt{\frac{\sigma_1}{\sigma_3}}, \quad (5)$$

where $f_{a1}^{WW} = (1 - f_{a2}^{WW} - f_{a3}^{WW} - f_{\Lambda 1}^{WW} - ...)$ is the effective fraction of the SM tree-level contribution, which is expected to dominate. The values of the effective cross section ratios are listed in Table 1.

Table 1: Table of cross section ratios for a 125.6 GeV Higgs boson used to convert effective fractions. Here σ_i is the effective cross-section of the process corresponding to $a_i = 1, a_{j\neq i} = 0$ in the $H \to WW \to \ell\nu\ell\nu$ final state.

Ratio	σ_1/σ_3	σ_1/σ_2	σ_1/σ_4
Value	3.01	1.25	1.87

For more exotic spin assignments of the new boson, a variety of tensor couplings is possible. In the case of the spin-one resonance, the scattering amplitude for its interaction with a pair of the massive V bosons consists of two independent terms and can be written as:

$$A(X_{J=1} \to VV) = b_1 \left[(\epsilon_1^* q)\,(\epsilon_2^* \epsilon_X) + (\epsilon_2^* q)\,(\epsilon_1^* \epsilon_X) \right] + b_2 \epsilon_{\alpha\mu\nu\beta} \epsilon_X^{\alpha} \epsilon_1^{*\mu} \epsilon_2^{*\nu} \tilde{q}^{\beta} \tag{6}$$

where ϵ_X is the polarization vector of the particle X. Here $b_1 \neq 0$ coupling corresponds to a vector particle, while $b_2 \neq 0$ coupling corresponds to a pseudovector particle. In the case of a general spin-two resonance and its interaction with a pair of W bosons, the scattering amplitude can be expressed in the following way:

$$\begin{aligned}
A(X_{J=2} \to V_1 V_2) = \Lambda^{-1} \Bigg[& 2c_1 t_{\mu\nu} f^{*1,\mu\alpha} f^{*2,\nu\alpha} + 2c_2 t_{\mu\nu} \frac{q_\alpha q_\beta}{\Lambda^2} f^{*1,\mu\alpha} f^{*2,\nu,\beta} \\
& + c_3 \frac{\tilde{q}^\beta \tilde{q}^\alpha}{\Lambda^2} t_{\beta\nu} (f^{*1,\mu\nu} f^{*2}_{\mu\alpha} + f^{*2,\mu\nu} f^{*1}_{\mu\alpha}) + c_4 \frac{\tilde{q}^\nu \tilde{q}^\mu}{\Lambda^2} t_{\mu\nu} f^{*1,\alpha\beta} f^{*(2)}_{\alpha\beta} \\
& + m_V^2 \left(2c_5 t_{\mu\nu} \epsilon_1^{*\mu} \epsilon_2^{*\nu} + 2c_6 \frac{\tilde{q}^\mu q_\alpha}{\Lambda^2} t_{\mu\nu} \left(\epsilon_1^{*\nu} \epsilon_2^{*\alpha} - \epsilon_1^{*\alpha} \epsilon_2^{*\nu} \right) + c_7 \frac{\tilde{q}^\mu \tilde{q}^\nu}{\Lambda^2} t_{\mu\nu} \epsilon_1^* \epsilon_2^* \right) \\
& + c_8 \frac{\tilde{q}^\mu \tilde{q}^\nu}{\Lambda^2} t_{\mu\nu} f^{*1,\alpha\beta} \tilde{f}^{*(2)}_{\alpha\beta} + c_9 t^{\mu\alpha} \tilde{q}_\alpha \epsilon_{\mu\nu\rho\sigma} \epsilon_1^{*\nu} \epsilon_2^{*\rho} q^\sigma \\
& + \frac{c_{10} t^{\mu\alpha} \tilde{q}_\alpha}{\Lambda^2} \epsilon_{\mu\nu\rho\sigma} q^\rho \tilde{q}^\sigma \left(\epsilon_1^{*\nu} (q \epsilon_2^*) + \epsilon_2^{*\nu} (q \epsilon_1^*) \right) \Bigg] ,
\end{aligned} \tag{7}$$

The c_1 and c_5 couplings correspond to parity-conserving interaction of a spin-2 tensor with the minimal couplings.

Assuming that the chiral symmetry is exact in the limit when fermion masses vanish, the general scattering amplitude that describes the interaction of the Higgs-like boson with fermions is

$$A(X_{J=0} f \bar{f}) = \frac{m_f}{v} \bar{u}_2 \left(\rho_1 + \rho_2 \gamma_5 \right) u_1 , \tag{8}$$

where m_f is the fermion mass and $\bar{u}_2$ and u_1 are the Dirac spinors. The two constants ρ_1 and ρ_2 correspond to the scalar and pseudo-scalar couplings. $q\bar{q}$ production of a spin-0 resonance is suppressed, but this is not the case for higher spins. For higher spins:

$$A(X_{J=1} f \bar{f}) = \epsilon^\mu \bar{u}_2 \left(\gamma_\mu \left(\rho_1^{(1)} + \rho_2^{(1)} \gamma_5 \right) + \frac{m_f \tilde{q}_\mu}{\Lambda^2} \left(\rho_3^{(1)} + \rho_4^{(1)} \gamma_5 \right) \right) u_1 , \tag{9}$$

$$A(X_{J=2} f \bar{f}) = \frac{1}{\Lambda} t^{\mu\nu} \bar{u}_2 \left(\gamma_\mu \tilde{q}_\nu \left(\rho_1^{(2)} + \rho_2^{(2)} \gamma_5 \right) + \frac{m_f \tilde{q}_\mu \tilde{q}_\nu}{\Lambda^2} \left(\rho_3^{(2)} + \rho_4^{(2)} \gamma_5 \right) \right) u_1 . \tag{10}$$

The $\rho_1^{(1)}$ ($\rho_2^{(1)}$) coupling corresponds to parity-conserving interaction of a vector (pseudo-vector). The $\rho_1^{(2)}$ ($\rho_2^{(2)}$) couplings correspond to parity-conserving interaction of a spin-2 tensor (pseudo-tensor). However, in practice in the $q\bar{q} \to X \to W^+W^-$ production and decay, there is no observable difference between the $\rho_1^{(J)}$ and $\rho_2^{(J)}$ couplings in $q\bar{q}$ production.

In Table 2 all the spin-0, 1, 2 scenarios explored in the analysis are shown. Mixed states of spin-0 are not shown but are considered in the analysis for the measurement of the continuous parameters. The subscripts m (minimal couplings) and h (couplings with higher-dimension operators) distinguish different scenarios. When certain coupling is indicated as non-zero, any value would produce equivalent results. In the case of $q\bar{q}$ production, $\rho_i^{(J)}$ couplings are assumed to be the same for all quark flavors.

Table 2: List of analysis scenarios of the production and decay of an exotic X particle with quantum numbers J^P. The subscripts m (minimal couplings) and h (couplings with higher-dimension operators) distinguish different scenarios. When certain coupling is indicated as non-zero, any value would produce equivalent results. In the case of $q\bar{q}$ production, $\rho_i^{(J)}$ couplings are assumed to be the same for all quark flavors.

J^P	mode	production couplings	decay couplings
0^+_m	$gg \to X \to \mathrm{W}^+\mathrm{W}^-$	(any) $a_2^{(0)} \neq 0$	$a_1^{(0)} \neq 0$
0^+_h	$gg \to X \to \mathrm{W}^+\mathrm{W}^-$	(any) $a_2^{(0)} \neq 0$	$a_2^{(0)} \neq 0$
$0^+_{\Lambda 1}$	$gg \to X \to \mathrm{W}^+\mathrm{W}^-$	(any) $a_2^{(0)} \neq 0$	$\Lambda_1 \neq \infty$
0^-	$gg \to X \to \mathrm{W}^+\mathrm{W}^-$	(any) $a_3^{(0)} \neq 0$	$a_3^{(0)} \neq 0$
1^+	$q\bar{q} \to X \to \mathrm{W}^+\mathrm{W}^-$	$\rho_2^{(1)}$ or $\rho_1^{(1)} \neq 0$	$b_2 \neq 0$
1^-	$q\bar{q} \to X \to \mathrm{W}^+\mathrm{W}^-$	$\rho_1^{(1)}$ or $\rho_2^{(1)} \neq 0$	$b_1 \neq 0$
2^+_m	$gg \to X \to \mathrm{W}^+\mathrm{W}^-$	$c_1 \neq 0$	$c_1 = c_5 \neq 0$
2^+_{h2}	$gg \to X \to \mathrm{W}^+\mathrm{W}^-$	$c_2 \neq 0$	$c_2 \neq 0$
2^+_{h3}	$gg \to X \to \mathrm{W}^+\mathrm{W}^-$	$c_3 \neq 0$	$c_3 \neq 0\,\mathrm{i}$
2^+_h	$gg \to X \to \mathrm{W}^+\mathrm{W}^-$	$c_4 \neq 0$	$c_4 \neq 0$
2^+_b	$gg \to X \to \mathrm{W}^+\mathrm{W}^-$	$c_1 \neq 0$	$c_1 \ll c_5 \neq 0$
2^+_{h6}	$gg \to X \to \mathrm{W}^+\mathrm{W}^-$	$c_1 \neq 0$	$c_6 \neq 0$
2^+_{h7}	$gg \to X \to \mathrm{W}^+\mathrm{W}^-$	$c_1 \neq 0$	$c_7 \neq 0$
2^-_h	$gg \to X \to \mathrm{W}^+\mathrm{W}^-$	$c_8 \neq 0$	$c_8 \neq 0$
2^-_{h9}	$gg \to X \to \mathrm{W}^+\mathrm{W}^-$	$c_8 \neq 0$	$c_9 \neq 0$
2^-_{h10}	$gg \to X \to \mathrm{W}^+\mathrm{W}^-$	$c_8 \neq 0$	$c_{10} \neq 0$
2^+_m	$q\bar{q} \to X \to \mathrm{W}^+\mathrm{W}^-$	$\rho_1^{(2)}$ or $\rho_2^{(2)} \neq 0$	$c_1 = c_5 \neq 0$
2^+_{h2}	$q\bar{q} \to X \to \mathrm{W}^+\mathrm{W}^-$	$\rho_1^{(2)}$ or $\rho_2^{(2)} \neq 0$	$c_2 \neq 0$
2^+_{h3}	$q\bar{q} \to X \to \mathrm{W}^+\mathrm{W}^-$	$\rho_1^{(2)}$ or $\rho_2^{(2)} \neq 0$	$c_3 \neq 0$
2^+_h	$q\bar{q} \to X \to \mathrm{W}^+\mathrm{W}^-$	$\rho_1^{(2)}$ or $\rho_2^{(2)} \neq 0$	$c_4 \neq 0$
2^+_b	$q\bar{q} \to X \to \mathrm{W}^+\mathrm{W}^-$	$\rho_1^{(2)}$ or $\rho_2^{(2)} \neq 0$	$c_1 \ll c_5 \neq 0$
2^+_{h6}	$q\bar{q} \to X \to \mathrm{W}^+\mathrm{W}^-$	$\rho_1^{(2)}$ or $\rho_2^{(2)} \neq 0$	$c_6 \neq 0$
2^+_{h7}	$q\bar{q} \to X \to \mathrm{W}^+\mathrm{W}^-$	$\rho_1^{(2)}$ or $\rho_2^{(2)} \neq 0$	$c_7 \neq 0$
2^-_h	$q\bar{q} \to X \to \mathrm{W}^+\mathrm{W}^-$	$\rho_1^{(2)}$ or $\rho_2^{(2)} \neq 0$	$c_8 \neq 0$
2^-_{h9}	$q\bar{q} \to X \to \mathrm{W}^+\mathrm{W}^-$	$\rho_1^{(2)}$ or $\rho_2^{(2)} \neq 0$	$c_9 \neq 0$
2^-_{h10}	$q\bar{q} \to X \to \mathrm{W}^+\mathrm{W}^-$	$\rho_1^{(2)}$ or $\rho_2^{(2)} \neq 0$	$c_{10} \neq 0$

3 Data and Simulated Samples

The data and the simulated samples for the SM backgrounds are the same as for the main $H \to W^+W^- \to \ell^+\nu\ell^-\bar{\nu}$ analysis [5] while new signal samples are introduced specifically for this analysis.

A dedicated simulation program JHUGen [10, 11, 13] is used to describe various final states in the production and decay to two vector bosons of the spin-0, 1, and 2 resonances in hadron-hadron collisions. For the spin-1 and 2 resonances, implementation of the processes $gg/q\bar{q} \to X \to W^+W^- \to 4f$ is incorporated into a simulation program which allows the general couplings of the X particle to gluons and quarks in production and to vector bosons in decay and includes all the spin correlations and interferences of all contributing amplitudes. For a spin-0 resonance, NLO QCD effects in the gluon fusion production through POWHEG event generators are introduced. Production of a spin-0 particle in vector-boson-fusion (VBF) and associated VH production (V=W,Z) is also modeled with spin correlations of associated particles. Simulation is interfaced to parton shower simulation as well as full detector simulation through the Les Houches Event file format.

Spin-0 signal samples were generated for $gg \to$ H, VBF, VH, and $t\bar{t}$H production, but contribution of $t\bar{t}H$ events is found to be negligible in this analysis. The analysis is designed to study anomalous couplings in the $H \to W^+W^-$ decay.

Simulated spin-0 scenarios include SM Higgs boson 0^+, pseudo-scalar 0^-, scalar with higher order corrections, 0_h^+, and $0_{\Lambda 1}^+$, as well as mixed samples where parameters have been varied, such as f_{a2}^{WW}=0.5, f_{a3}^{WW}=0.5, and $f_{\Lambda 1}^{WW}$=-0.5. In order to increase the statistics of the simulated samples for each hypothesis studies, the MELA package [15] was adopted to re-weight any $H \to WW$ sample to model any other spin-0 sample, leading to an order of magnitude increase in statistics for further analysis.

For spin-1, two $q\bar{q} \to X$ samples have been produced, the exotic pseudo-vector 1^+, and the exotic vector 1^-. An additional mixed sample with $f_{b2} = 0.5$ has also been produced. The spin-1 hypotheses are considered under the assumption that the resonance decaying into W^+W^- is not necessarily the same resonance observed in the $H \to \gamma\gamma$ channel, as $J = 1$ in the latter case is prohibited by the Landau-Yang theorem. For spin-2, a variety of gg and $q\bar{q}$ scenarios have been produced, including tensor with higher dimension operators 2_h^+ and pseudo-tensor 2_h^-. See Table 2 for the list of models considered.

4 Event Selection

The objects, event selection and background estimation, are exactly the same as in the legacy paper of the $H \to W^+W^-$ channel [5]. The treatment of the systematic uncertainties is also identical. This analysis introduces several new signal samples produced explicitly for this study and presented in section 3 without further modification on the analysis.

Final states with two leptons, a substantial amount of $E_{\mathrm{T}}^{\mathrm{miss}}$, and either 0 or 1 jets, are studied. Signal events are produced mainly by gluon-fusion, providing a clear signature not accompanied by hadronic activity (0 jets). The VBF and VH production fraction is very small, below 10% and no particular optimization of the selection has been made for these cases.

The particle flow algorithm [16] is used to reconstruct all observable particles in the event.

Events are selected if they have exactly one electron and one muon, with opposite charge, passing the full identification and isolation criteria presented in [5]. The leading lepton should

have $p_{\mathrm{T}} > 20$ GeV, and for the second one $p_{\mathrm{T}} > 10$ GeV is required. Only electrons (muons) with $|\eta|$ <2.5 (2.4) are considered. Events are classified according to the number of selected jets that fulfil $E_{\mathrm{T}} > 30$ GeV and $|\eta| < 4.7$.

The $e\mu$ pair is then required to have an invariant mass above 12 GeV, and a p_{T} above 30 GeV.

A *projected* $E_{\mathrm{T}}^{\mathrm{miss}}$ variable is employed to further select signal events. It is defined as the component of $E_{\mathrm{T}}^{\mathrm{miss}}$ transverse to the nearest lepton if the difference in azimuth between this lepton and the $E_{\mathrm{T}}^{\mathrm{miss}}$ vector is less than $\pi/2$. If there is no lepton within $\pi/2$ of the direction of $E_{\mathrm{T}}^{\mathrm{miss}}$ in azimuth, $E_{\mathrm{T}}^{\mathrm{miss}}$ is used directly. Since the *projected* $E_{\mathrm{T}}^{\mathrm{miss}}$ resolution is degraded by pile-up, the minimum of two $E_{\mathrm{T}}^{\mathrm{miss}}$ observables is used: the first includes all reconstructed particles in the event, while the second uses only the charged particles associated with the primary vertex. Events with *projected* $E_{\mathrm{T}}^{\mathrm{miss}}$ above 20 GeV are selected for the analysis.

Data-driven corrections are applied to simulation as described in [5].

Two variables are used to define the signal region, the invariant mass of the $e\mu$ pair, m_{ll}, and the transverse mass m_T. The signal region is defined by $m_{ll} < 200$ GeV, and $60 \leq m_T \leq 280$ GeV. The distribution of this variables for data and expected SM Higgs signal and backgrounds are presented in figure 1.

Two-dimensional $m_{ll} - m_T$ templates are built and used as input of the statistical procedure. The templates for background and data are the same as the ones used in [5]. For illustrative purposes templates for SM Higgs boson and 2_b^+ are presented in Figure 2

New templates for SM Higgs boson and alternative J^P modes are used to perform the study. The shapes of the variables used in the templates are similar for VBF and WH component, the main VH production mode, with respect to $gg \to$ H.

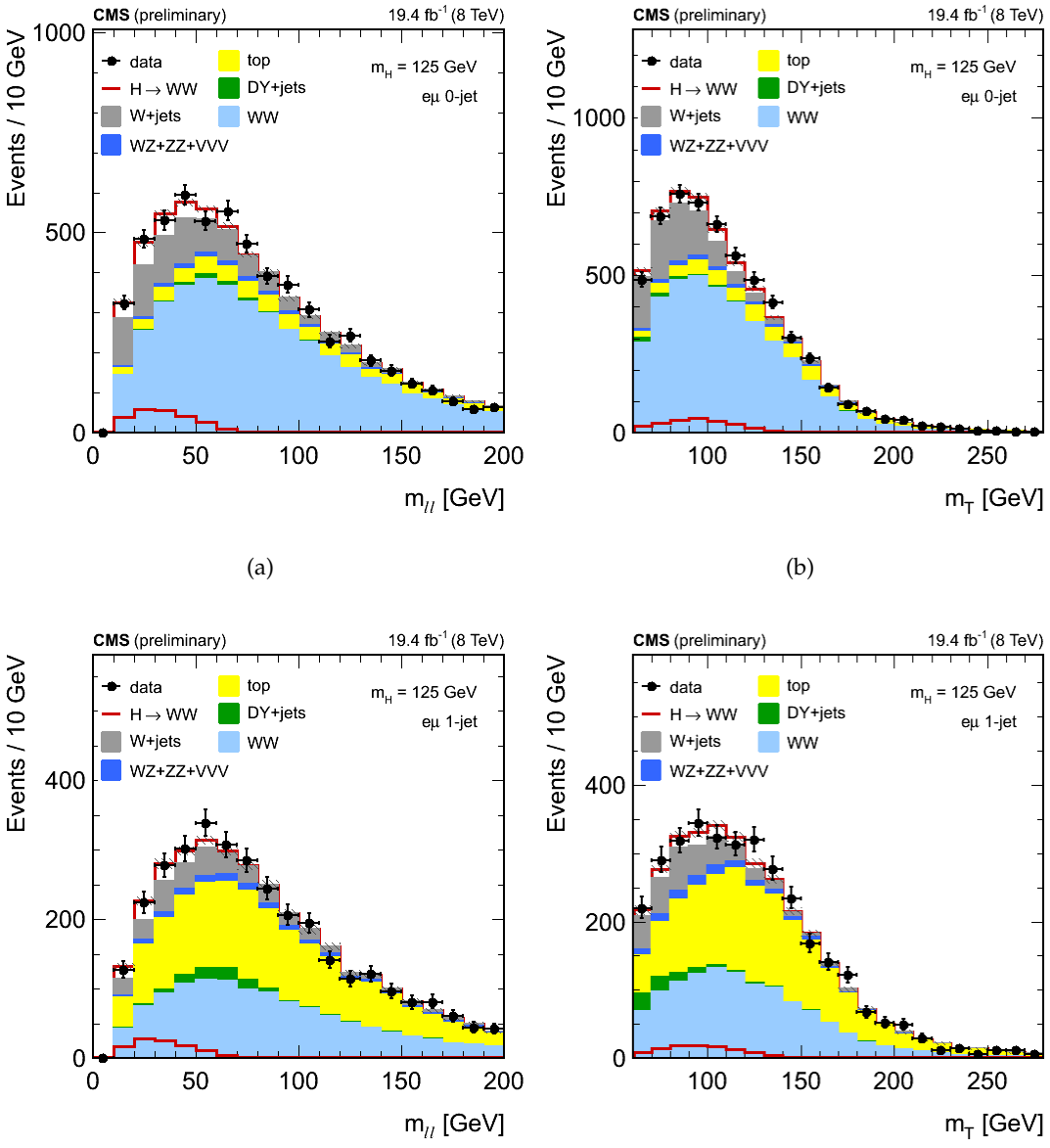

(a) (b)

(c) (d)

Figure 1: Distributions of m_{ll} and m_T for data and expected SM Higgs signal and backgrounds for events with 0 jets (Upper row) and 1 jet (Lower row).

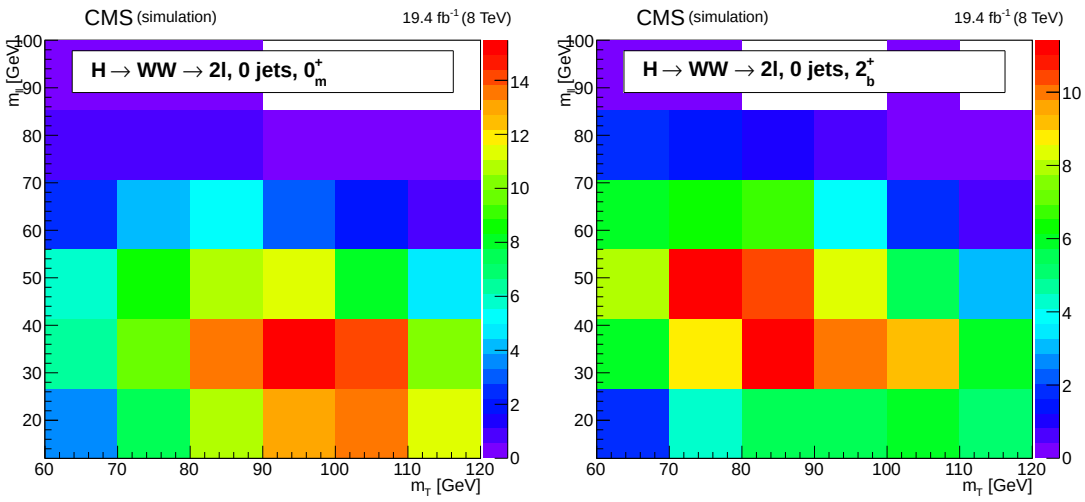

(a) (b)

Figure 2: Two-dimensional templates of m_{ll} and m_T for SM Higgs boson 0^+_m (a) and 2^+_b (b).

5 Parameter estimation

To extract the anomalous coupling parameters $\vec{\zeta} = \{f_{a2}^{WW}, f_{a3}^{WW}, f_{\Lambda 1}^{WW}\}$, a binned maximum likelihood fit is performed to the selected events. The overall likelihood for N bins is

$$\mathcal{L} = \prod_{i}^{N} \frac{\left(n_i^{\text{sig}}(\vec{\zeta}) + n_i^{\text{bkg}}\right)^{n_i} e^{-n_i^{\text{sig}}(\vec{\zeta}) - n_i^{\text{bkg}}}}{n_i!} \tag{11}$$

n_i^{sig} and n_i^{bkg} are the number of expected signal and background events in the bin i, and n_i is the number of observed events from data. Both signal and background are obtained from full simulated events. The final signal yield is a function of the anomalous coupling parameters, $n_i^{\text{sig}}(\vec{\zeta})$. Considering f_{a2}^{WW} measurement for example, the signal yield is expressed in the following function

$$n_i^{sig}(f_{a2}^{WW}) = \mu[(1 - f_{a2}^{WW})\, n_i^{sig,0^+} + f_{a2}^{WW}\, n_i^{sig,0_h^+} \pm \sqrt{(1 - f_{a2}^{WW}) f_{a2}^{WW}}\, n_i^{int}] \tag{12}$$

$n_i^{sig,0^+}$ and $n_i^{sig,0_h^+}$ represent the expected number events from the a_1 and a_2 terms in the bin i, respectively, while n_i^{int} is predicted by the interference between a_1 and a_2 term. The sign of the interference is positive when ϕ_{a2} is 0 and negative when ϕ_{a2} is π. The signal strength μ is floated in the fit.

In the binned maximum likelihood fit, the coupling fractions is reated as parameter of interest. The systematics related to normalization and shape are profiled. A scan of the parameter of interest is performed to extract the 68% and 95% CL. Three parameters are measured for a spin-0 scenario: f_{a3}^{WW}, f_{a2}^{WW}, and $f_{\Lambda 1}^{WW}$.

The CP-odd cross-section fraction in the Higgs boson coupling to two vector bosons is represented by f_{a3}^{WW}. In [6], a first measurement of f_{a3}^{WW} in H $\to ZZ$ is presented, where any phase between the a_1 and a_3 couplings is considered. To measure f_{a3}^{WW}, the function described in Eq. 12 is parameterized using a SM Higgs boson 0_m^+ template, a pseudo-scalar 0^- template, and a template to represent their interference, extracted from a dedicated sample with $f_{a3}^{WW} = 0.5$.

Figure 3 shows the likelihood scan of f_{a3}^{WW}. The signal component of the likelihood of event i is:

$$\mathcal{L}^i_{f_{a3}^{WW}} = (1 - f_{a3}^{WW})\mathcal{L}^i_{0+} + f_{a3}^{WW}\mathcal{L}^i_{0-} + \sqrt{(1 - f_{a3}^{WW}) f_{a3}^{WW}}\,\mathcal{L}^i_{int} \tag{13}$$

The average expected and observed distribution of -2$ln\mathcal{L}$ as a function of f_{a3}^{WW} is presented. The 68% and 95% CL are represented by horizontal lines.The observed best fit value of f_{a3} is compatible with 0 (0.16σ away), and the pure pseudo-scalar model is 1.13σ deviated.

By definition f_{a3}^{WW} (and subsequently f_{a2}^{WW} and $f_{\Lambda 1}^{WW}$) is an amplitude square fraction, going from 0 to 1. Here, a real amplitude is considered, and the relative phase ϕ_{a3} is either 0 or π. In order to distinguish the two phase scenarios, $f_{a3}^{WW}\cos(\phi_{a3})$ is drawn from -1 to 1, where the negative side corresponds to phase π.

The scalar with higher-dimension operators in couplings to the vector bosons is represented by f_{a2}^{WW}. The fit parameterization is obtained using a 0_m^+ template, a 0_h^+ template, and a template to represent their interference, extracted from a dedicated sample with $f_{a2}^{WW} = 0.5$.

Figure 4 shows the likelihood scan of f_{a2}^{WW}. The signal component of the likelihood is of event i is:

$$\mathcal{L}^i_{f_{a2}^{WW}} = (1 - f_{a2}^{WW})\mathcal{L}^i_{0+m} + f_{a2}^{WW}\mathcal{L}^i_{0+h} + \sqrt{(1 - f_{a2}^{WW}) f_{a2}^{WW}}\,\mathcal{L}^i_{int} \tag{14}$$

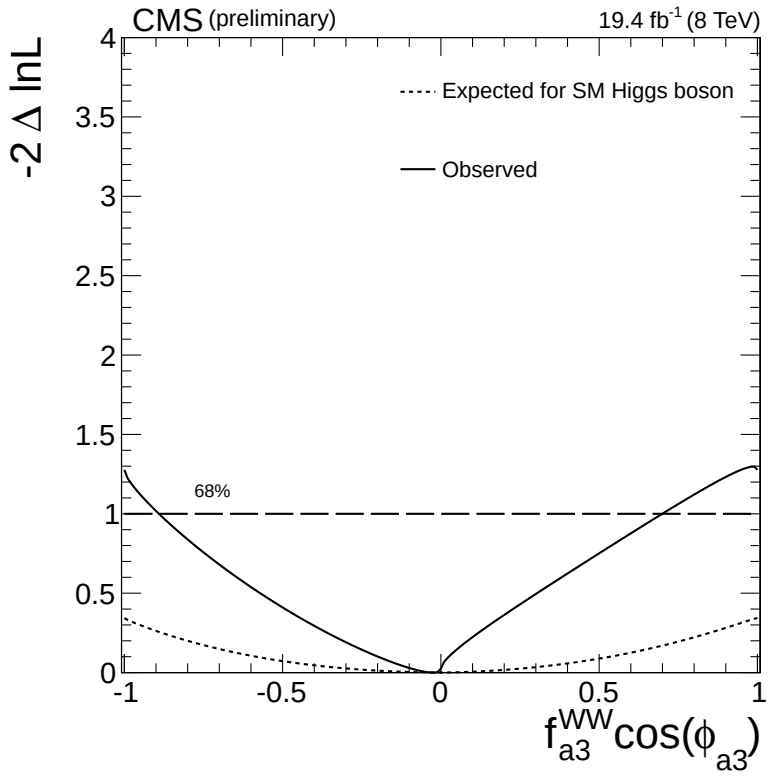

Figure 3: Average expected and observed distribution of $-2\Delta ln\mathcal{L}$ as a function of f_{a3}^{WW}. The 68% and 95% CL are represented by horizontal lines. The dashed curve represents the SM Higgs expectation, and the solid curve is the observed. The positive and negative side stands for $\phi = 0$ and $\phi = \pi$, respectively.

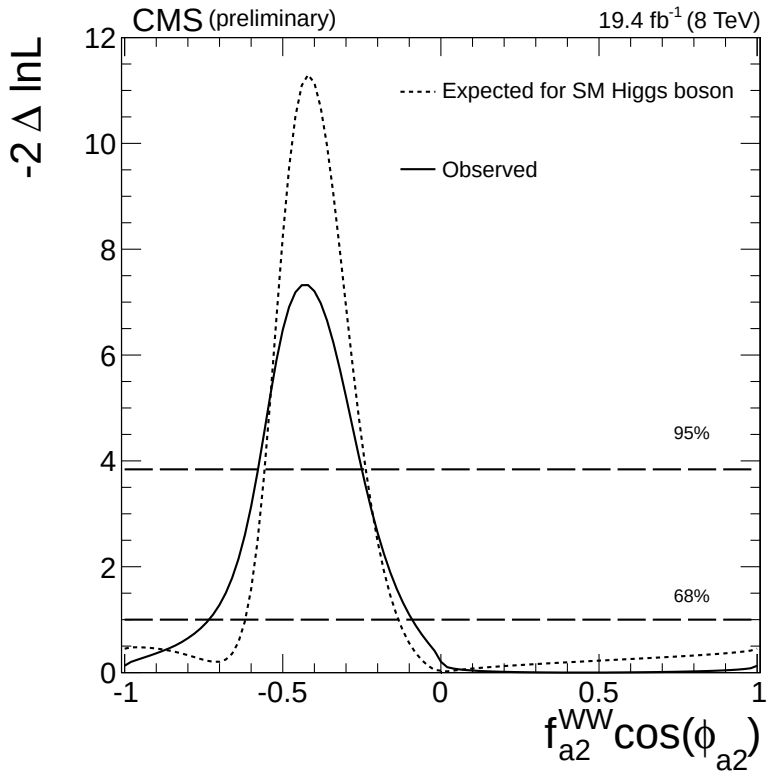

Figure 4: Average expected and observed distribution of $-2\Delta ln\mathcal{L}$ as a function of f_{a2}^{WW}. The 68% and 95% CL are represented by horizontal lines. The dashed curve represents the SM Higgs expectation, and the solid curve is the observed. The positive and negative side stands for $\phi = 0$ and $\phi = \pi$, respectively.

The average expected and observed distribution of -2$ln\mathcal{L}$ as a function of f_{a2}^{WW} is presented. The 68% and 95% CL are represented by horizontal lines. The presence of a strong interference between the SM and the anomalous coupling causes a very different kinematic around $f_{a2} = 0.5$, $\phi_{a2} = \pi$, which brings a large exclusion. The observed best fit value of f_{a2} is non-zero, but is still compatible with the SM within 0.45σ. The same shape of the likelihood as the expected is observed, where there is a large exclusion near $f_{a2}^{WW} = 0.5$, $\phi_{a2} = \pi$.

Finally, $f_{\Lambda 1}^{WW}$ represents the scalar with higher-dimension operators coupling to vector bosons, which otherwise has the same tensor structure as in the SM. Parameterization is obtained with a 0_m^+ template, a $f_{\Lambda 1}^{WW} = 1$ and $\phi_{\Lambda 1} = 0$ template, and a template to represent their interference, extracted from a dedicated sample with $f_{\Lambda 1}^{WW} = 0.5$, $\phi_{\Lambda 1} = \pi$.

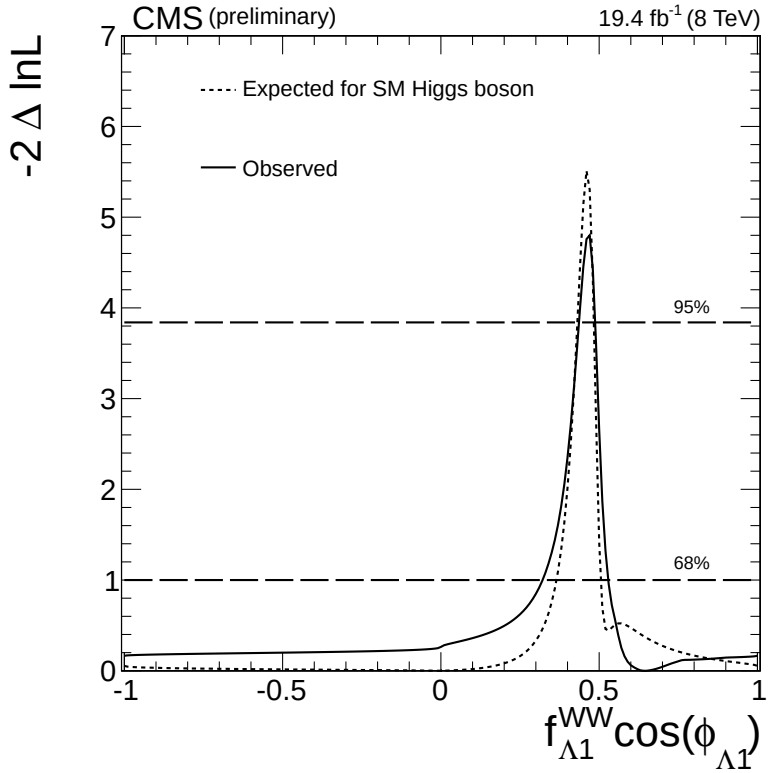

Figure 5: Average expected and observed distribution of $-2\Delta ln\mathcal{L}$ as a function of $f_{\Lambda 1}^{WW}$. The 68% and 95% CL are represented by horizontal lines. The dashed curve represents the SM Higgs expectation, and the solid curve is the observed. The positive and negative side stands for $\phi = 0$ and $\phi = \pi$, respectively.

Figure 5 shows the likelihood scan of $f_{\Lambda 1}^{WW}$. The signal component of the likelihood is of event i is:

$$\mathcal{L}^i_{\Lambda 1}{}^{WW} = (1 - f_{\Lambda 1}^{WW})\mathcal{L}^i_{0+m} + f_{\Lambda 1}^{WW}\mathcal{L}^i_{f_{\Lambda 1}=1} + \sqrt{(1 - f_{\Lambda 1}^{WW}) f_{\Lambda 1}^{WW}}\mathcal{L}^i_{int} \tag{15}$$

The average expected and observed distribution of -2$ln\mathcal{L}$ as a function of $f_{\Lambda 1}^{WW}$ is presented. The 68% and 95% CL are represented by horizontal lines. Similar to f_{a2} measurement, the strong destructive interference between the SM and the anomalous coupling around the $f_{\Lambda 1}^{WW} = 0.5$ region gives a much higher exclusion than other phase spaces. The observed best fit value of $f_{\Lambda 1}^{WW}$ is 0.31σ away from the SM. A high exclusion is observed in the same region as expected.

6 Hypotesis testing

In addition to the measurement of the spin-0 parameters f_{a3}^{WW}, f_{a2}^{WW}, and $f_{\Lambda 1}^{WW}$; spin-1 and spin-2 scenarios are also studied. Different pure spin hypothesis are compared with the SM Higgs boson 0^+. The comparison with spin-1 and spin-2 scenarios is performed in the same way that it was done for [5].

The yields of the different hypothesis are nominally taken from the simulated samples assuming the SM Higgs boson cross section. A signal-plus-background model is built for each hypothesis, based on the two-dimensional templates on $m_{ll} - m_T$, using the same bin widths and data selection as for the low m_H case described in [5]. The background templates are the same as in the SM Higgs boson search analysis.

For each hypothesis a binned maximum likelihood ($\mathcal{L}$) fit is performed, to simultaneously extract the signal strength and background contributions. This likelihood fit model is the same as in the SM Higgs boson search. Fits are performed for both models, and the likelihoods are calculated with the signal rates allowed to float independently for each signal type. The test statistic, $q = -2ln(\mathcal{L}_{J^P}/\mathcal{L}_{0_m^+})$, where $\mathcal{L}_{0_m^+}$ and $\mathcal{L}_{J^P}$ are the best fit likelihood values for the SM Higgs boson and the alternative hypothesis is then used to quantify the consistency of the two models with data. The expected separation between the two hypotheses is quoted in two scenarios, when events are generated with a-priori expectation for the signal yields ($\sigma/\sigma_{SM} = 1$) and when the signal strength is determined from the fit to data.

The observed separation quotes consistency of the observation with the 0_m^+ model or J^P model and corresponds to the scenario where σ/σ_{SM} is determined from the fit to data and are defined as the median of q expected for one hypothesis under the other hypothesis.

6.1 Spin-1

The results for the three spin-1 scenarios are shown in figure 6. The average separation between the SM Higgs boson and each alternative spin-1 hypothesis is larger than one standard deviation. The alternative spin-1 hypotheses are disfavored with CLs values of 3.9% for 1^-, 14.0% for 1^+, and 8.7% for 1_{mix}.

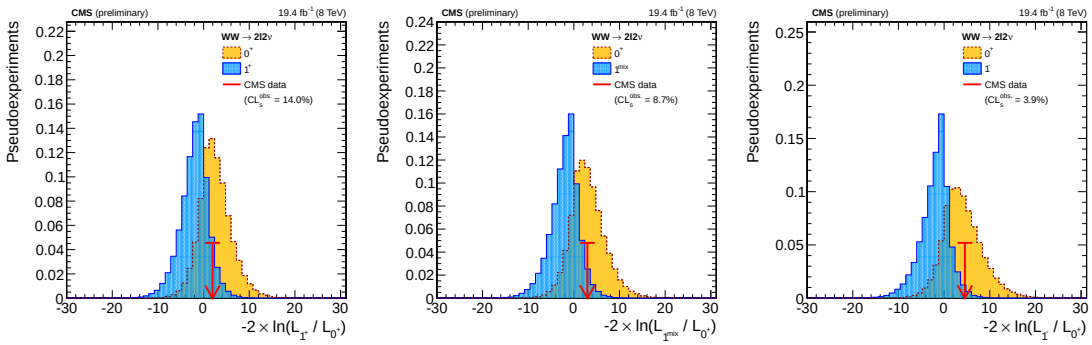

Figure 6: Distributions of $-2ln(L_{1^x}/L_{0_m^+})$, combining the 0-jet and 1-jet categories in the $e\mu$ final state, for the 1^+, 1^{Mix}, and 1^- hypotheses at $m_H = 125.6$ GeV. The distributions are produced using the signal strength determined from the fit to data. The observed value is indicated by the red arrow.

6.2 Spin-2

The results for the different spin-2 scenarios are shown assuming a $f_{q\bar{q}}$ fraction of 0% in figure 7. The median test statistic for the 0^+ and J = 2 hypotheses as well as its observed value, as a function of the $q\bar{q} \to$ H component, is presented in figure 8 for each of the scenarios tested. The results are obtained using the σ/σ_{SM} value determined from the fit to data.

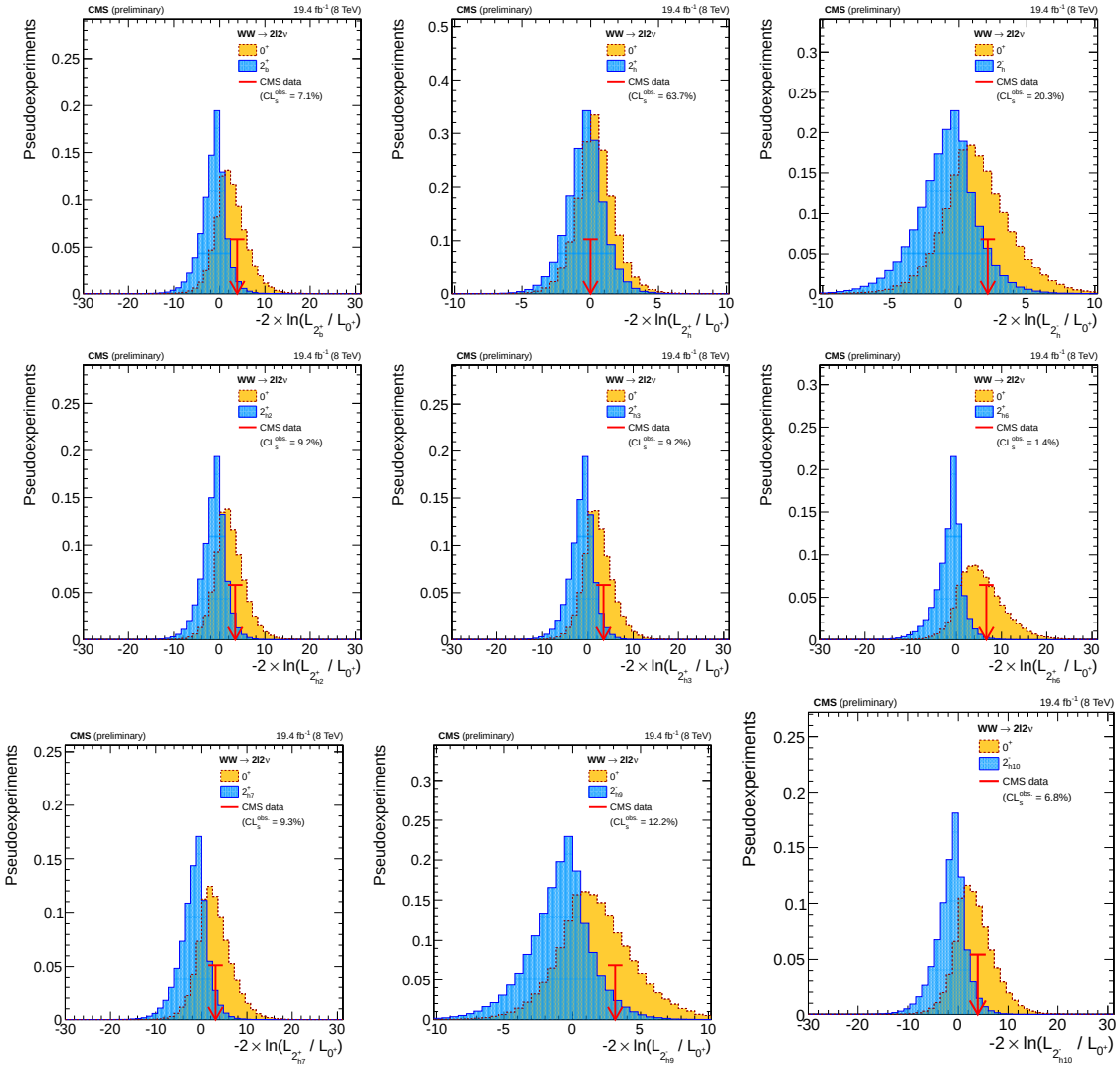

Figure 7: Distributions of $-2ln(L_2/L_{0_m^+})$, combining the 0-jet and 1-jet categories in the $e\mu$ final state, for the nine spin-2 hypotheses at $m_H = 125.6$ GeV. The distributions are produced using the signal strength determined from the fit to data. The observed value is indicated by the red arrow. The distributions are shown for the case $f_{q\bar{q}} = 0$.

In all cases the data favor the SM hypothesis with respect to the alternative hypothesis. The alternative hypothesis The alternative hypothesis 2_b^+ is excluded at a 92.9% (100%) CL or higher for $f_{q\bar{q}}$ 0% (100%). Other hypothesis for which H $\to$ W^+W^- achieves a good discrimination are 2_{h2}^+, excluded at a 90.8% (100%) CL or higher for $f_{q\bar{q}}$ 0% (100%); or 2_{h3}^+.

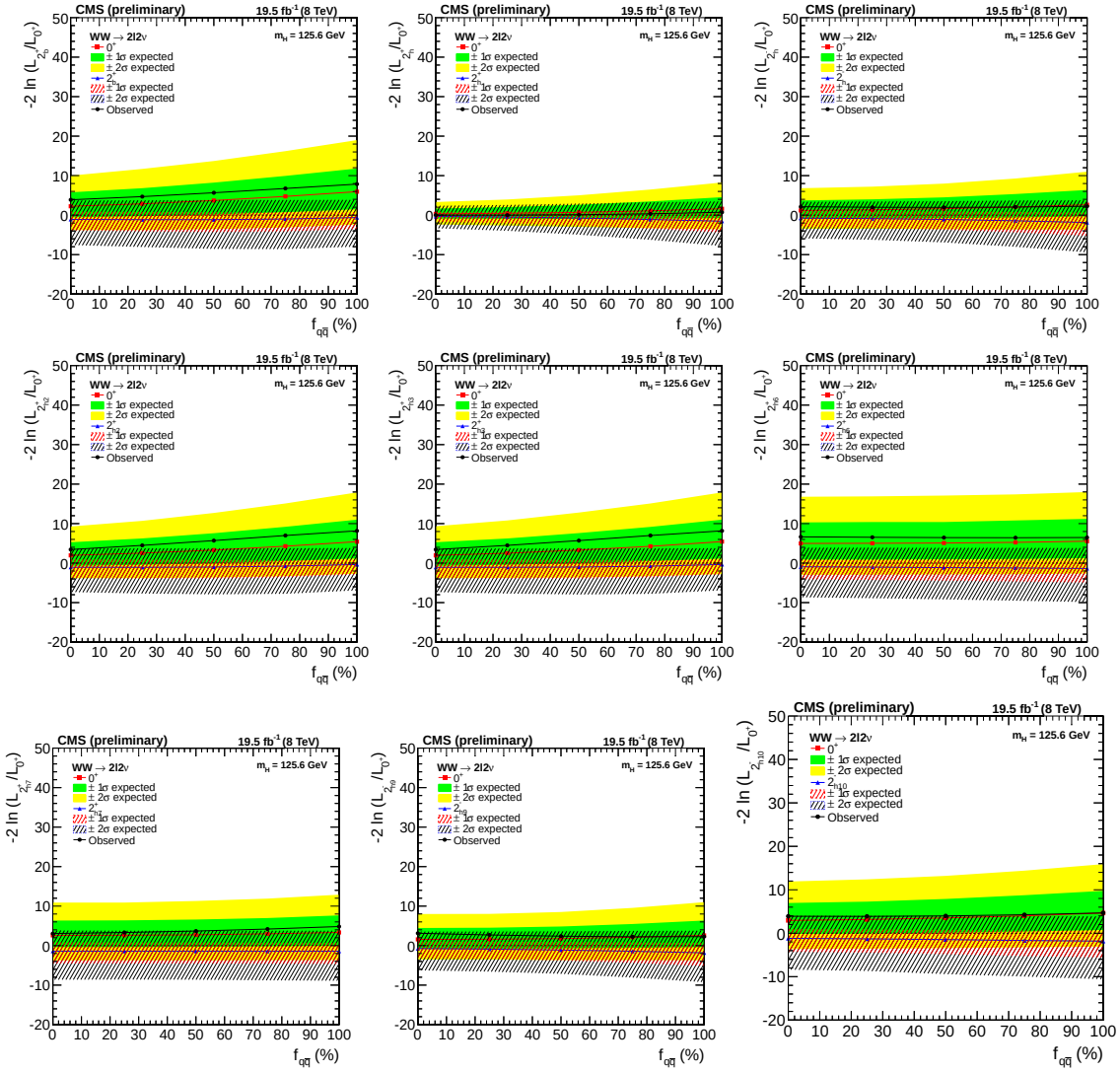

Figure 8: Observed and expected median test statistic for the 0^+ and J $= 2$ hypotheses, as a function of the $f_{q\bar{q}}$ fraction for each of the spin-2 models tested using the σ/σ_{SM} value determined from the fit to data.

7 Results

An extension of the studies on the spin parity of the Higgs boson performed in [5] is presented using the full 8 TeV proton-proton collision dataset recorded by the CMS experiment at the LHC. The analysis chain, data, backgrounds, systematic treatment, and framework is left untouched. Several simulated samples with alternative spin-0, 1 and 2 scenarios are generated.

For spin-0 scenarios, the first measurement of the parameters f_{a3}^{WW}, f_{a2}^{WW}, and $f_{\Lambda 1}^{WW}$, in $H \to W^+W^-$ decays is presented. The measurements, performed taking into account interference effects, are summarized in table 3. The 68% and 95% CL for f_{a2}^{WW} and $f_{\Lambda 1}^{WW}$ could be quoted, but the f_{a3}^{WW} is not reaching 68% yet all over the range.

Agreement with the SM expectations is observed. The fraction of a CP-odd contribution to the decay amplitude, expressed through the fraction f_{a3}^{WW} of the corresponding decay rate is consistent with the expectation for the SM Higgs boson, as well as f_{a2}^{WW} and $f_{\Lambda 1}^{WW}$. The best fit values for the three parameters are within less than 0.4σ from the SM expectation. The observed best fit value of f_{a3}^{WW} is compatible with 0 (0.16σ away), and the pure psuedo-scalar model is excluded at 1.13σ. The observed best fit value of f_{a2} is non-zero, but is still compatible with the SM within 0.45σ. The observed best fit value of $f_{\Lambda 1}^{WW}$ is 0.31σ away from the SM. The $H \to W^+W^-$ channel is not sensitive enough on its own to measure the experimental value of these parameters, however, when combined with $H \to ZZ$ there is a sizeable improvement on the sensitivity.

For pure spin-1 and 2 scenarios, the alternative hypotheses are compared to a SM Higgs boson. In the later case, the results are obtained as a function of the $q\bar{q} \to H$ component. When this fraction is equal to 100%, a maximal separation is achieved in all the scenarios, the minimal separation is obtained when this fraction is 0% and the exotic scenarios are more similar to the mostly gg-produced SM Higgs boson. For spin-2, the results corresponding to $f_{q\bar{q}} = 0\%$ and $f_{q\bar{q}} = 100\%$ are shown. Table 4 presents a summary of the results of the hypothesis testing.

A preference for a scalar SM Higgs boson with spin 0_m^+ is observed, in all cases the data favors the SM hypothesis with respect to the alternative hypothesis. The average separation between the SM Higgs boson and each alternative spin-1 hypothesis is larger than one standard deviation. The alternative spin-1 hypotheses are disfavored with CLs values of 3.9% for 1^-, 14.0% for 1^+, and 8.7% for 1_{mix}.

Table 3: Summary of the observed and expected limits of the f_{a3}^{WW}, f_{a2}^{WW}, $f_{\Lambda 1}^{WW}$parameters for spin-0, under the assumption that all the couplings are real. Unless otherwise specified the other amplitudes are assumed to be the SM prediction. The confidence intervals are extracted from the asymptotic properties of the $-2\Delta ln\mathcal{L}$ distribution (at $-2\Delta ln\mathcal{L}$ = 3.84) and have an approximate coverage of 95%.

	Observed and expected limits @95%CL (real couplings)	
Parameter	Expected	Observed
f_{a3}	–	–
f_{a2}	$-0.56 < f_{a2}cos(\phi_{a2}) < -0.24$	$-0.58 < f_{a2}cos(\phi_{a2}) < -0.25$
$f_{\Lambda 1}$	$0.43 < f_{\Lambda 1}cos(\phi_{\Lambda 1}) < 0.48$	$0.44 < f_{\Lambda 1}cos(\phi_{\Lambda 1}) < 0.49$

The alternative hypothesis 2_b^+ is excluded at a 92.9% (100%) CL or higher for $f_{q\bar{q}}$ 0% (100%). Other hypothesis for which $H \to W^+W^-$ achieves a good discrimination are 2_{h2}^+, excluded at a 90.8% (100%) CL or higher for $f_{q\bar{q}}$ 0% (100%); or 2_{h3}^+. Other scenarios are more complicated to separate from a SM Higgs boson, like 2_h^+, for which the expected and observed separation is smaller than one standard deviation. The summary of the spin-1 and spin-2 results is also

Table 4: Summary of the models used in the analysis of the spin and parity hypotheses. The expected separation is quoted for two scenarios, where the value of σ/σ_{SM} for each hypothesis is determined from the fit to data and where events are generated with $\sigma/\sigma_{SM} = 1$. The observed separation quotes consistency of the observation with the 0^+_m model or J^P model and corresponds to the scenario where σ/σ_{SM} is determined from the fit to data. The last column quotes the CLs value that defines the minimum confidence level (1 - CLs) at which the J^P model is excluded.

J^P model	J^P production	Expected ($\sigma/\sigma_{SM} = 1$)	Observed 0^+	Observed J^P	CLs
1^-	$q\bar{q} \to$ H	1.8σ (2.9σ)	-0.2σ	2.1σ	3.9%
1_{Mix}	$q\bar{q} \to$ H	1.6σ (2.6σ)	-0.1σ	1.7σ	8.7%
1^+	$q\bar{q} \to$ H	1.5σ (2.3σ)	0.1σ	1.4σ	14.0%
2^+_b	$gg \to$ H ($f_{q\bar{q}} = 0\%$)	1.4σ (2.4σ)	-0.5σ	2.0σ	7.1%
2^+_h	$gg \to$ H ($f_{q\bar{q}} = 0\%$)	0.6σ (1.1σ)	0.3σ	0.3σ	63.7%
2^-_h	$gg \to$ H ($f_{q\bar{q}} = 0\%$)	1.0σ (2.0σ)	-0.4σ	1.5σ	20.3%
2^+_{h2}	$gg \to$ H ($f_{q\bar{q}} = 0\%$)	1.3σ (2.3σ)	-0.5σ	1.9σ	9.2%
2^+_{h3}	$gg \to$ H ($f_{q\bar{q}} = 0\%$)	1.3σ (2.3σ)	-0.5σ	1.9σ	9.2%
2^+_{h6}	$gg \to$ H ($f_{q\bar{q}} = 0\%$)	2.0σ (2.2σ)	-0.3σ	2.6σ	1.4%
2^+_{h7}	$gg \to$ H ($f_{q\bar{q}} = 0\%$)	1.5σ (2.3σ)	-0.1σ	1.7σ	9.3%
2^-_{h9}	$gg \to$ H ($f_{q\bar{q}} = 0\%$)	1.1σ (2.1σ)	-0.6σ	1.8σ	12.2%
2^-_{h10}	$gg \to$ H ($f_{q\bar{q}} = 0\%$)	1.6σ (2.8σ)	-0.3σ	1.9σ	6.8%
2^+_b	$q\bar{q} \to$ H ($f_{q\bar{q}} = 100\%$)	2.2σ (3.4σ)	-0.3σ	2.8σ	0.7%
2^+_h	$q\bar{q} \to$ H ($f_{q\bar{q}} = 100\%$)	1.3σ (1.9σ)	0.4σ	1.0σ	25.3%
2^-_h	$q\bar{q} \to$ H ($f_{q\bar{q}} = 100\%$)	1.6σ (2.5σ)	0.1σ	1.5σ	11.7%
2^+_{h2}	$q\bar{q} \to$ H ($f_{q\bar{q}} = 100\%$)	2.1σ (3.2σ)	-0.5σ	2.9σ	0.7%
2^+_{h3}	$q\bar{q} \to$ H ($f_{q\bar{q}} = 100\%$)	2.1σ (3.2σ)	-0.5σ	2.9σ	0.6%
2^+_{h6}	$q\bar{q} \to$ H ($f_{q\bar{q}} = 100\%$)	2.2σ (3.3σ)	-0.2σ	2.5σ	1.3%
2^+_{h7}	$q\bar{q} \to$ H ($f_{q\bar{q}} = 100\%$)	1.7σ (2.7σ)	-0.4σ	2.2σ	3.7%
2^-_{h9}	$q\bar{q} \to$ H ($f_{q\bar{q}} = 100\%$)	1.6σ (2.5σ)	0.1σ	1.5σ	11.5%
2^-_{h10}	$q\bar{q} \to$ H ($f_{q\bar{q}} = 100\%$)	2.1σ (3.2σ)	-0.01σ	2.1σ	3.2%

presented in Figure 9. There is a correlation between the different results that is due to the fact that the variables used are the same in all the scenarios, the data is also the same, as well as the SM Higgs hypothesis.

All the results are consistent with the results presented in [14] for H $\to ZZ$ and with the SM expectations for a SM Higgs boson.

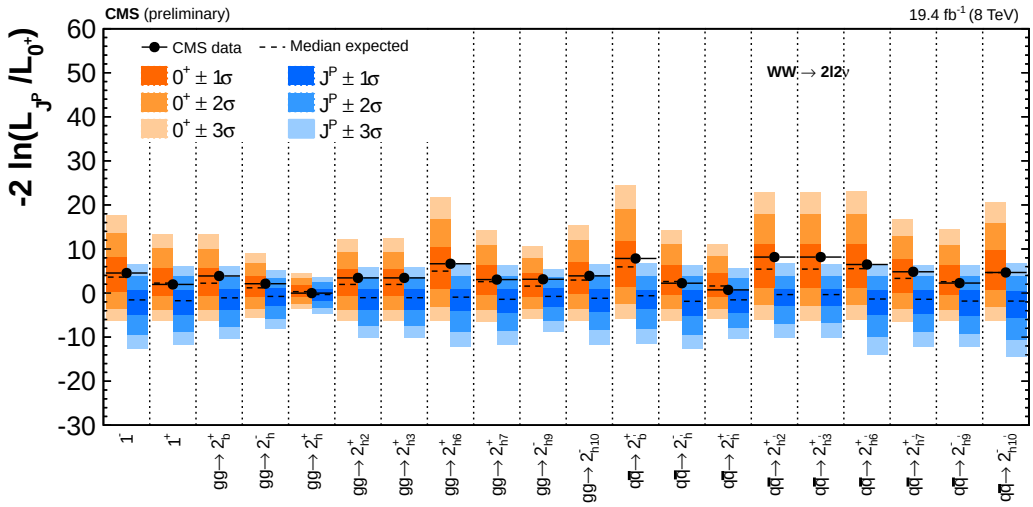

Figure 9: Summary of the expected and observed values for the test-statistic q distributions for the alternative spin-one and spin-two hypotheses tested with respect to the SM Higgs boson. The orange (blue) bands represent the 1σ, 2σ, and 3σ around the median expected value for the SM Higgs boson hypothesis (alternative hypothesis). The black points represents the observed value.

References

[1] ATLAS Collaboration, "Observation of a new particle in the search for the Standard Model Higgs boson with the ATLAS detector at the LHC", *Phys.Lett.* **B716** (2012) 1–29, doi:10.1016/j.physletb.2012.08.020, arXiv:1207.7214.

[2] CMS Collaboration, "Observation of a new boson at a mass of 125 GeV with the CMS experiment at the LHC", *Phys.Lett.* **B716** (2012) 30–61, doi:10.1016/j.physletb.2012.08.021, arXiv:1207.7235.

[3] CMS Collaboration, "Observation of a new boson with mass near 125 GeV in pp collisions at $\sqrt{s}$ = 7 and 8 TeV", *JHEP* **1306** (2013) 081, doi:10.1007/JHEP06(2013)081, arXiv:1303.4571.

[4] CMS Collaboration Collaboration, "On the mass and spin-parity of the Higgs boson candidate via its decays to Z boson pairs", *Phys.Rev.Lett.* **110** (2013) 081803, arXiv:1212.6639.

[5] CMS Collaboration, "Measurement of Higgs boson production and properties in the WW decay channel with leptonic final states", *JHEP* **1401** (2014) 096, doi:10.1007/JHEP01(2014)096, arXiv:1312.1129.

[6] CMS Collaboration, "Measurement of the properties of a Higgs boson in the four-lepton final state", doi:10.1103/PhysRevD.89.092007, arXiv:1312.5353.

[7] J. R. Dell'Aquila and C. A. Nelson, "Simple Tests for CP or P Violation by Sequential Decays: V1 V2 Modes With Decays Into $\bar{\ell}$epton (A) $\ell(B)$ And/or $\bar{q}$ (A) $q(B)$", *Phys.Rev.* **D33** (1986) 101, doi:10.1103/PhysRevD.33.101.

[8] D. Chang, W.-Y. Keung, and I. Phillips, "CP odd correlation in the decay of neutral Higgs boson into Z Z, W+ W-, or t anti-t", *Phys.Rev.* **D48** (1993) 3225–3234, doi:10.1103/PhysRevD.48.3225, arXiv:hep-ph/9303226.

[9] E. Accomando et al., "Workshop on CP Studies and Non-Standard Higgs Physics", arXiv:hep-ph/0608079.

[10] Y. Gao et al., "Spin determination of single-produced resonances at hadron colliders", *Phys.Rev.* **D81** (2010) 075022, doi:10.1103/PhysRevD.81.075022, arXiv:1001.3396.

[11] S. Bolognesi et al., "On the spin and parity of a single-produced resonance at the LHC", *Phys.Rev.* **D86** (2012) 095031, doi:10.1103/PhysRevD.86.095031, arXiv:1208.4018.

[12] P. Artoisenet et al., "A framework for Higgs characterisation", *JHEP* **1311** (2013) 043, doi:10.1007/JHEP11(2013)043, arXiv:1306.6464.

[13] I. Anderson et al., "Constraining anomalous HVV interactions at proton and lepton colliders", *Phys.Rev.* **D89** (2014) 035007, doi:10.1103/PhysRevD.89.035007, arXiv:1309.4819.

[14] CMS Collaboration, "Constrains on anomalous HVV interactions using $H4l$ decays", *HIG-14-014* (2014).

[15] http://www.pha.jhu.edu/spin/.

[16] CMS Collaboration, "Particle–Flow Event Reconstruction in CMS and Performance for Jets, Taus, and $E_{\mathrm{T}}^{\mathrm{miss}}$", CMS Physics Analysis Summary CMS-PAS-PFT-09-001, 2009.